Title:

100 kHz Yb-fiber laser pumped 3 µm optical parametric amplifier for probing solid state systems in the strong field regime

Authors:

Giedre Marija Archipovaite, Stéphane Petit, Jean-Christophe Delagnes, Eric Cormier

Final manuscript

The original publication may be found at:

Journal: Optics Letters 42, 891-894 (2017)

DOI: https://doi.org/10.1364/OL.42.000891

100 kHz Yb-fiber laser pumped 3 µm optical parametric amplifier for probing solid state systems in the strong field regime

GIEDRE MARIJA ARCHIPOVAITE, STÉPHANE PETIT, JEAN-CHRISTOPHE DELAGNES*, ERIC CORMIER

Université Bordeaux-CNRS-CEA-UMR 5107, Centre Lasers Intenses et Applications, 351 Cours de la Liberation, F-33405 Talence, France
**Corresponding author: jean-christophe.delagnes@u-bordeaux.fr*

Received XX Month XXXX; revised XX Month, XXXX; accepted XX Month XXXX; posted XX Month XXXX (Doc. ID XXXXX); published XX Month XXXX

We report on a laser source operating at 100 kHz repetition rate and delivering 8 µJ few cycles midIR pulses at 3 µm. The system is based on Optical Parametric Amplification (OPA) pumped by high repetition rate Yb-doped femtosecond fiber chirped amplifier (FCPA). This high-intensity ultrafast system is a promising tool for strong-field experiments (up to 50 GV/m and 186 T) in low ionization potential atomic and molecular systems, or solid state physics with coincidence measurements. As a proof of principle, up to the 6th harmonic have been generated in 1 mm zinc selenide (ZnSe) sample. © 2017 Optical Society of America

OCIS codes: *(190.4970) Parametric oscillators and amplifiers; (320.7110) Ultrafast nonlinear optics; (140.3070) Infrared and far-infrared lasers.*

http://dx.doi.org/XX.XXXX/XX.XX.XXXXXX

Few-cycle ultrashort pulse light sources in the near- to middle-infrared (midIR) at longer wavelength (2-12 µm) are in high demand for strong field physics in atoms, molecules or condensed matter. Indeed, various applications such as bright and coherent soft X-ray generation [1], conventional or multidimensional spectroscopy [2], ultrafast magnetism [3] requires such devices. The λ^2.I scaling law inherent to the high order harmonic generation (HHG) process favors longer driving wavelengths in order to produce more energetic XUV photons, and potentially shorter attosecond, soft X-ray pulses [1]. Unfortunately, photon energy extension is at the cost of an efficiency drop scaling as $\lambda^{-5.5}$ [4]. Here, the availability of a high-repetition rate laser system is paramount to mitigate the efficiency issue and still produce high photon fluxes. Even though there are only a few laser gain medium suitable for intense femtosecond pulse generation in the midIR spectral region the overall scalability of pulse repetition rate, duration and power is still a challenge [5,6]. To cite a few, 4-cycle pulses were achieved in graphene mode locked Cr:ZnSe at 2.4 µm with an output power of 250 mW and pulse energy of 2.3 nJ [7]. In an amplified architecture 300 µJ pulses were generated in Cr:ZnSe at the repetition rate of 1 kHz with a pulse duration of 300 fs [8]. The fiber technology is also able to produce midIR radiation where, for instance, 207 fs pulses at 2.8 µm were generated in Er doped fluoride glass fiber laser providing peak powers up to 3.5 kW [9].
An alternative approach to simultaneously generate high-energy short pulses in the midIR region is based on nonlinear frequency conversion by means of three-wave mixing in a second order susceptibility crystal. In the present context, the processes of difference frequency generation (DFG) and optical parametric amplification (OPA) are commonly implemented.
Several high-power chirped pulse optical parametric amplification (OPCPA) systems in the wavelength region of interest have been reported. A four-stage 160 kHz OPCPA delivers 20 µJ, 55 fs pulses at 3.05 µm [10], a three-stage 50 kHz system with 44.2 fs, 21.8 µJ at 3.4 µm [11], another three-stage OPCPA delivering 10 µJ, 72 fs at 3070 nm with the repetition rate of 125 kHz [12]. These systems are based on periodically poled lithium niobate (PPLN) crystals. However, lithium niobate (LN) and PPLN crystals are known to introduce beam distortions when applied to high power conditions, to exhibit parasitic phase matching and to have a lower damage threshold. On the other hand, KTA crystals could be successfully used as an alternative [13,14].
In this letter we present a combined system where a chirped PPLN (cPPLN) crystal is used for efficient 3 µm generation and KTA stages for amplification. A similar approach is also demonstrated in [15], but there, the main focus is on the signal beam at 1.55 µm in a non-collinear configuration leading to an angularly disperse idler wave at 3 µm. As in [12], our system is based on a fiber CPA system delivering fs pulses as compared to the other systems where the pulse duration is ranging from 10 ps [10,11] down to 1 ps [14]. Femtosecond fiber lasers have shown their capabilities for strong field experiments by demonstrating coherent XUV emission at unprecedented adjustable repetition rate reaching up to the MHz level [16]. Since then, femtosecond fiber laser performances

have continuously increased to reach for instance peak powers of 46 GW with an energy of 12 mJ [17]and durations reduced down to 2 cycles [18]. Here, we intend to take advantage of the unique properties of FCPA systems to extent their capabilities to longer wavelengths by pumping few cycle optical parametric amplifiers and generate intense fields in the midIR.

With the emerging sub-ps pumped few cycle OPCPA systems working further in the midIR and the lack of broadband seed sources in this spectral region, the importance of coherent seeding radiation such as white light continuum (WLC) generation is also arising. However, there are just a few reports of WLC generation in bulk materials, when pumped by mid-IR sources. Most common materials tested are bulk YAG, Sapphire, CaF_2 and BaF_2 [19–21]. In [22], spectral broadening in zinc selenide (ZnSe) is demonstrated when the pump source is tuned 0.8 – 2.4 μm and in [23] white light continuum is generated when pumping with few optical cycle pulses at 1.85 μm. There authors also compare the peak power required for WLC generation in different materials and the threshold for ZnSe is shown to be the lowest. Seeing zinc selenide as a promising material, we have examined the applicability of it in order to generate WLC at longer wavelengths (3 μm), where also high harmonics were generated and the source was proved to be suitable for solid state physics in strong field regime experiments.

The scheme of our three-stage optical parametric amplifier (OPA) is depicted in Fig. 1.a. The system is pumped by high repetition rate home built fiber chirped pulse amplifier (FCPA), which delivers 350 fs pulses with a pulse energy of 290 μJ and a repetition rate of 100 kHz.

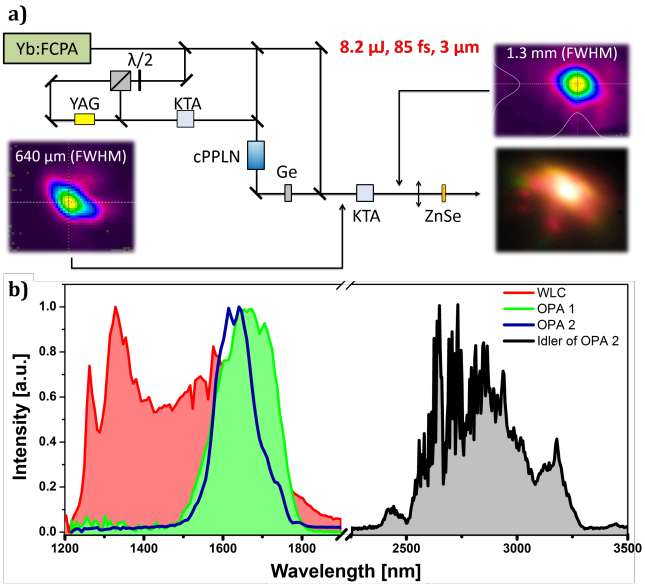

Fig. 1. a) Scheme of a three-stage OPA, delivering 85 fs pulses at 3 μm. The insets show the spatial profiles measured before and after the third stage. The output of the system is collimated and suitable for intense field physics experiments such as harmonic generation in polycrystalline ZnSe (transmitted beam picture shown in inset) b) Typical spectra (normalized) of the WLC and amplification in the first two stages.

A white light continuum (WLC) is generated by filamentation in a 15 mm yttrium aluminum garnet (YAG) rod and the reddest fraction of the broadened spectrum seeds the OPAs. A careful inspection of the focusing conditions shows an optimum for the focal length f' forming the filament (f'=250 mm for 0.22 μJ at 1030 nm). Indeed, longer wavelengths can be obtained when a rather loose focusing (longer Rayleigh range) is chosen. There, a longer filament is formed and the broadening process develops smoothly. This configuration allows generation of spectra extending higher into the infrared (2.2 μm in our case) compared to tight focusing. The ability to directly amplify WLC in the infrared side yields the possibility to circumvent loss of efficiency due to visible OPA stage, which should be pumped by the second harmonic and may lead to angularly dispersed idler beam. When starting from the visible WLC part, two main methods can be applied in order to reach the midIR region. First, using an amplified WLC as a pump beam in a 2nd OPA stage, but the process is not very efficient. Secondly, amplifying the broadband idler pulses in the 2nd OPA stage. However, in order to generate broad idler a noncollinear phase matching is performed in the 1st OPA stage which results in angularly chirped idler generation. With direct IR seeding, the pump is thus more efficiently converted, while carrier envelope phase (CEP) stability is achieved by passing through fewer stages than when starting from the visible part of the continuum.

The first OPA stage consists of 6 mm potassium titanyl arsenate (KTA) crystal. 40 μJ of pump is focused by 300 mm lens and reach peak intensity of about 0.5 TW/cm^2; white light continuum is imaged into the crystal with a 50 mm achromatic lens. Beam sizes of pump and signal beams at the crystal are 80 μm and 70 μm respectively. A 200 nm broadband spectrum at 1.6-1.7 μm is amplified in a noncollinear configuration with the internal angle between pump and signal beams of 2.5°. The signal is amplified up to 60 nJ.

In the second OPA stage a 7.4 mm long cPPLN crystal (HC Photonics Corp.) with the poling period linearly chirped from 28.4 to 31 μm is used and signal from the first stage is amplified. Here, CPPLN crystal was chosen due to a broader and flat spectral gain profile and limited back conversion comparing with PPLN crystals [24] and a d_{eff} more than 10 times higher than a KTA crystal. The collinear configuration allows generation of angular chirp free idler pulses, which are later amplified in the last OPA stage. 40 μJ of pump is used and the WLC is further amplified up to 2 μJ and 0.75 μJ of idler at 3 μm are generated. The efficiency in this stage is 4% and gain is 33. Typical spectra of the first two stages are depicted in Fig. 1 (b).

In the last OPA stage, the idler pulses generated in the previous stage are collinearly amplified in a 10 mm length KTA crystal. While the (PP)LN used in the second stage provided an ultrabroad bandwidth and important gain, KTA has been chosen here for the last power stage in spite of its smaller d_{eff}. Indeed, due its thermal, mechanical and optical properties, a KTA based architecture can achieve better performances when scaling the average and peak power up, and thus circumvent the limitations due to heating (4 times less absorption), damage threshold (1.5 times higher) encountered with LN that exhibit damage under the same high-average, high-peak power regime. Moreover KTA has a smaller group velocity mismatch (GVM) between pump, signal and idler, along with a reduced group delay dispersion (GDD) as compared with LN (about half in both cases). These last characteristics make KTA more suitable for ultrashort compressed pulse amplification. The incoming seed signal for this stage is collimated and focused by a –500 mm ROC and a –1000 mm ROC silver mirrors, while the

pump beam is focused by +750 mm lens. The pump focus is shifted after the crystal in order to control the overlap between the pump and the seed spot sizes which are measured to be around 420 μm (FWHM) and 640 μm (FWHM) respectively (see Fig1 a). Peak intensity of pump pulses is 0.1 TW/cm^2. The mismatch between the spot sizes is set on purpose in order to extract the maximum energy from the pump beam, to suppress any potential superfluorescence due to weak seeding at the sides of the beam and to increase the spatial beam quality by selecting the central part of the seed for amplification. The amplified signal is afterwards collimated by a – 500mm ROC silver mirror with a beam diameter of 1.3 mm (FWHM).

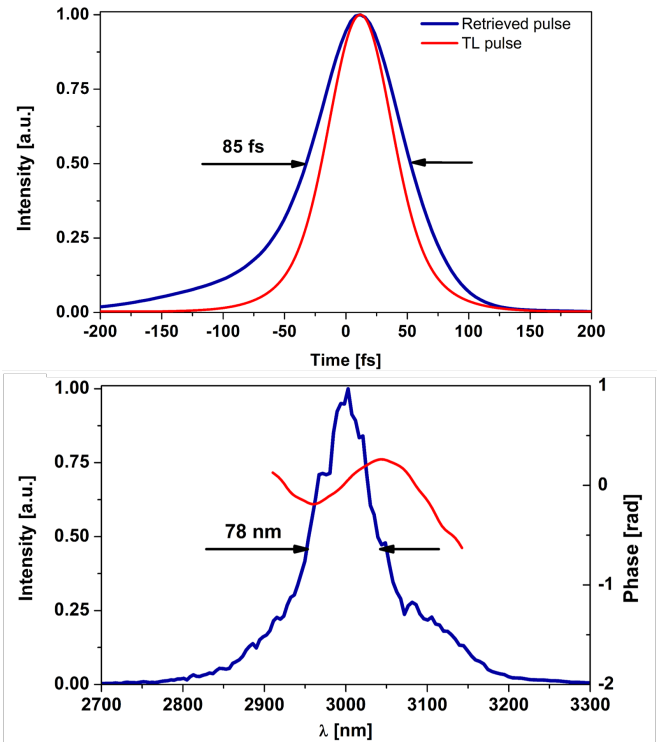

Fig. 2. Temporal (top) and spectral (bottom) characterization of the midIR pulses. Pulses of 85 fs are retrieved for a transform limited duration of 64 fs.

In order to separate the seed of the third stage from the residual pump and signal beams after the OPA 2, a 3 mm uncoated germanium filter is inserted. The transmission of the filter for the idler wave is 45%, so only 330 nJ of seed is injected in the amplifier. The remaining laser energy (130 μJ) is used to pump the last stage and the signal is amplified up to 8.2 μJ. The maximum level of superfluorescence is estimated by blocking the seed and measuring the pulse energy, which is about 200 nJ (2.5 %) and is likely to decrease when amplification process takes place. The efficiency of the amplification in this stage is 6.3% and gain is 25. The overall efficiency of the system, energy conversion from total pump into the idler beam is 2.8%, which is similar to the other high repetition rate set-ups 2% [10] and 4.5% [11]. When the energy of the pump pulses for the last stage was set to 200 μJ, 15 uJ (7.5 % stage efficiency) pulses at 3 μm were achieved with slight changes in the spectral and temporal characteristics as described below.

The temporal pulse profile has been measured with a home built second harmonic (SH) frequency-resolved optical gating (FROG) device. The SH signal is generated in a 400 μm thick $AgGaS_2$ (AGS) crystal and the spectrograms are recorded with a NIRQuest 256 (Ocean Optics) spectrometer.

Table 1. Summary of dispersion properties of materials used for the post compression of OPA3 output pulses.

Material	ϕ_2, fs^2 [25]	ϕ_2/ϕ_3 (ϕ_3, fs^3)	τ_{pulse}, fs
4 mm YAG	-1108	-0.15 (7452)	82
1 mm CaF_2	-92	-0.18 (507)	69
2 mm ZnSe	340	0.4 (846)	70
5 mm ZnSe	850		70
3 mm Ge	4782	0.5 (9780)	413
None	-	-	62

Different materials were added in the 3 μm beam in order to compress the pulses to the shortest value after the last amplification stage. The results obtained from FROG measurements are summarized in Table 1. This experiment was done under lower power and tighter focusing conditions; the shortest pulse duration was 62 fs. After the optimization of the amplification stage for the best compromise between power and duration, pulses of 85 fs (64 fs transform limited) have been characterized (see Fig.2). The germanium filter inserted between the OPA 2 and OPA 3 provides sufficient group velocity dispersion (GVD) in the way that the output of the OPA3 is optimally compressed, even though the spectral phase shows the presence of third order dispersion, which also introduces an asymmetry of the temporal pulse profile. All the dispersion management is done with bulk materials, so the third order dispersion could not be completely compensated. The CEP stability is intrinsically implemented, since WLC and OPA stages are pumped by the same single laser source.

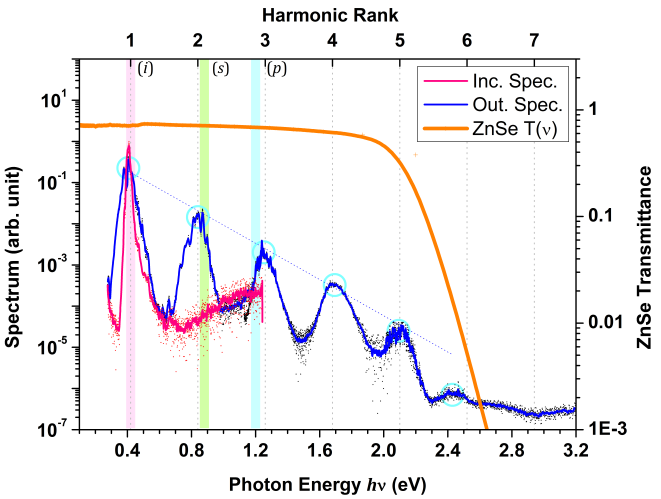

Fig. 3. Spectral broadening and generation of harmonics in 1 mm of ZnSe, up to 6th harmonics is observed. (i), (s) and (p) bars correspond to idler signal and pump wavelengths range.

With those characteristics of energy, duration and beam quality, intensities can reach typically 10^{12} to several 10^{13} W/cm^2. When

the output of the OPA3 is focused by a -200 mm ROC silver mirror, the spot size is evaluated to be about 200 µm (FWHM) leading to a pulse peak intensity of 0.3 TW/cm^2. The peak electric field F is in this case ~1 GV/m. Such strong electric field is likely to generate broadband continuum, light filament, as well as high-order-harmonic (HOH) in solids. MidIR ultrashort pulses based on bulk kHz laser systems have already been used for HHG in solids such as ZnO [26] and ZnSe [27,28]. For the sake of comparison with our fiber-based 100 kHz architecture, we used 1 mm of polycrystalline ZnSe sample.

Within our experimental conditions the peak power P_p=96 MW is more than twice higher than the critical power P_c=40 MW required for filamentation. When focusing the beam, a polychromatic dotted pattern [29] was observed at the output of the ZnSe sample that is due to the polycrystalline nature associated with higher nonlinear effects. Besides filamentation, we also expect to observe HOH. Indeed, for ZnSe (bandgap E_g=2.7 eV) interacting with the 3 µm pulse described above, the Keldysh parameter $\gamma=\omega\sqrt{m^* E_g}/q_e F$ [30] is evaluated to ~0.4. We have thus recorded the output spectrum displayed in Fig. 3. The initial spectrum is broadened and covered the region from 2 to 4.3 µm (0.3 – 0.6 eV). The spectrum clearly shows a decaying periodic structure whose peaks are identified as high harmonics of the driving field. As a result of the non-centrosymmetry of ZnSe odd and even order up to 6th harmonic are observed (limited by the bandgap of ZnSe). The first three unabsorbed harmonics are produced with about 8, 1.2, and 0.3 % respectively, decreasing with a power ∝-2.2. HOH below the ZnSe bandgap have also been reported in ref. 27. Due to a longer pump wavelength (3.9 µm), up to the 7th harmonic was generated at the repetition rate of 1 kHz and 200 fs pulse duration with a slightly steeper slope. The fact, that we achieve similar results tends to prove that the sample doesn't undergo any thermal effects due to high repetition rate laser. Moreover the 100 kHz repetition rate and beam quality of our source results in a bright harmonic emission as compared with bulk solid-state kHz systems enhancing significantly the signal over noise ratio.

In summary, we demonstrated a fiber laser pumped, passively CEP stabilized 3 µm OPA, which delivers 8 µJ pulses with the duration of 85 fs. This system is potentially tunable in the 2.4 - 3.6 µm range. Finally this middle infrared ultrafast source has been designed for solid state physics in the non-perturbative regime. Further development will shorten the pulse to few cycle with a CEP stability control, and an increase of the energy to 50 µJ. With the present characteristics, our first demonstration of HOH in ZnSe by a fiber laser pumped OPA shows how fiber lasers based systems are already very promising tools for future work such as band structure investigation [31], strong field Bloch oscillations, or HOH dynamics beyond the band gap of semi-conductors.

Funding. Laserlab-Europe IV ILAT (EU-H2020 654148), the ANR (ANR-10-IDEX-03-02), the ANR-ASTRID (ANR-15-ASTR-0005) and ELI-ALPS GOP-1.1.1-12/B-2012-0001.

Acknowledgments. The authors would like to thank Henri Bachau, and Patrick Martin for fruitful discussions, and HC Photonics Corp for their help in designing the cPPLN.

References

1. M.-C. Chen, C. Mancuso, C. Hernández-García, F. Dollar, B. Galloway, D. Popmintchev, P.-C. Huang, B. Walker, L. Plaja, A. A. Jaroń-Becker, A. Becker, M. M. Murnane, H. C. Kapteyn, and T. Popmintchev, Proc. Natl. Acad. Sci. **111**, E2361–E2367 (2014).
2. R. M. Hochstrasser, Proc. Natl. Acad. Sci. U. S. A. **104**, 14190–14196 (2007).
3. C. Boeglin, E. Beaurepaire, V. Halté, V. López-Flores, C. Stamm, N. Pontius, H. A. Dürr, and J.-Y. Bigot, Nature **465**, 458–61 (2010).
4. A. D. Shiner, C. Trallero-Herrero, N. Kajumba, H. C. Bandulet, D. Comtois, F. Légaré, M. Giguère, J. C. Kieffer, P. B. Corkum, and D. M. Villeneuve, Phys. Rev. Lett. **103**, 1–4 (2009).
5. I. T. Sorokina, V. V. Dvoyrin, N. Tolstik, and E. Sorokin, IEEE J. Sel. Top. Quantum Electron. **20**, 99 -110 (2014).
6. S. B. Mirov, V. V. Fedorov, D. Martyshkin, I. S. Moskalev, M. Mirov, and S. Vasilyev, IEEE J. Sel. Top. Quantum Electron. **21**, 292-310 (2015).
7. N. Tolstik, E. Sorokin, and I. T. Sorokina, Opt. Express **22**, 5564–71 (2014).
8. P. Moulton and E. Slobodchikov, in *CLEO:2011 - Laser Applications to Photonic Applications* (OSA, 2011), p. PDPA10.
9. S. Duval, M. Bernier, V. Fortin, J. Genest, M. Piche, and R. Vallee, Optica **2**, 623–626 (2015).
10. M. Baudisch, H. Pires, H. Ishizuki, T. Taira, M. Hemmer, and J. Biegert, J. Opt. **17**, 94002 (2015).
11. B. W. Mayer, C. R. Phillips, L. Gallmann, and U. Keller, Opt. Express **22**, 20798–808 (2014).
12. P. Rigaud, A. Van De Walle, M. Hanna, N. Forget, F. Guichard, Y. Zaouter, K. Guesmi, F. Druon, and P. Georges, Opt. Express **24**, 26494–26502 (2016).
13. M. Baudisch, M. Hemmer, H. Pires, and J. Biegert, Opt. Lett. **39**, 5802–5805 (2014).
14. G. Andriukaitis, T. Balčiūnas, S. Ališauskas, A. Pugžlys, A. Baltuška, T. Popmintchev, M.-C. Chen, M. M. Murnane, and H. C. Kapteyn, Opt. Lett. **36**, 2755–7 (2011).
15. M. Mero, F. Noack, F. Bach, V. Petrov, and M. J. J. Vrakking, Opt. Express **23**, 33157 (2015).
16. J. Boullet, Y. Zaouter, J. Limpert, S. Petit, Y. Mairesse, B. Fabre, J. Higuet, E. Mével, E. Constant, and E. Cormier, Opt. Lett. **34**, 1489–1491 (2009).
17. M. Kienel, M. Müller, A. Klenke, J. Limpert, and A. Tünnermann, Opt. Lett. **41**, 3343 (2016).
18. S. Hädrich, M. Kienel, M. Müller, A. Klenke, J. Rothhardt, R. Klas, T. Gottschall, T. Eidam, A. Drozdy, P. Jójárt, Z. Várallyay, E. Cormier, K. Osvay, A. Tünnermann, and J. Limpert, Opt. Lett. **41**, 4332–4335 (2016).
19. A E. Dormidonov, V. O. Kompanets, S. V Chekalin, and V. P. Kandidov, Opt. Express **23**, 29202–10 (2015).
20. F. Silva, D. R. Austin, A. Thai, M. Baudisch, M. Hemmer, D. Faccio, A. Couairon, and J. Biegert, Nat. Commun. **3**, 807 (2012).
21. S. Ališauskas, D. Kartashov, A. Pugzlys, D. Faccio, A. Zheltikov, A. Voronin, and A. Baltuska, in *CLEO: 2013* (OSA, 2013), p. QW1E.6.
22. M. Durand, A. Houard, K. Lim, A. Durécu, O. Vasseur, and M. Richardson, Opt. Express **22**, 5852–5858 (2014).
23. A. Choudhuri, A. Ruehl, N. Dipalo, I. Leon, I. Hartl, R. J. D. Miller, and J. Biegert, , https://doi.org/10.1364/CLEO_QELS.2016.FF1M.2(2016).
24. L. Gallmann, "Sources and techniques for attosecond science," ETH Zurich (2011).
25. M. N. Polyanskiy, http://refractiveindex.info/about.php.
26. S. Ghimire, A. D. DiChiara, E. Sistrunk, P. Agostini, L. F. DiMauro, and D. A. Reis, Nat. Phys. **7**, 138–141 (2011).
27. A. H. Chin, O. G. Calderón, and J. Kono, Phys. Rev. Lett. **86**, 3292–3295 (2001).
28. T. Kanai, P. Malevich, S. Kangaparambil, H. Hoogland, R. Holzwarth, A. Pugzlys, and A. Baltuska, in *Conference on Lasers and Electro-Optics*, OSA Technical Digest (2016) (Optical Society of America, 2016), paper STu3I.2.
29. T. D. Chinh, W. Seibt, and K. Siegbahn, J. Appl. Phys. **90**, 2612 (2001).
30. L. V. Keldysh, Sov. Phys. JETP **20**, 1307–1314 (1965).
31. G. Vampa, T. J. Hammond, N. Thiré, B. E. Schmidt, F. Légaré, C. R. McDonald, T. Brabec, D. D. Klug, and P. B. Corkum, Phys. Rev. Lett. 115, 193603 (2015).

Full references:

1. M.-C. Chen, C. Mancuso, C. Hernández-García, F. Dollar, B. Galloway, D. Popmintchev, P.-C. Huang, B. Walker, L. Plaja, A. A. Jaroń-Becker, A. Becker, M. M. Murnane, H. C. Kapteyn, and T. Popmintchev, "Generation of bright isolated attosecond soft X-ray pulses driven by multicycle midinfrared lasers," Proc. Natl. Acad. Sci. **111**, E2361–E2367 (2014).
2. R. M. Hochstrasser, "Two-dimensional spectroscopy at infrared and optical frequencies.," Proc. Natl. Acad. Sci. U. S. A. **104**, 14190–14196 (2007).
3. C. Boeglin, E. Beaurepaire, V. Halté, V. López-Flores, C. Stamm, N. Pontius, H. A. Dürr, and J.-Y. Bigot, "Distinguishing the ultrafast dynamics of spin and orbital moments in solids," Nature **465**, 458–61 (2010).
4. A. D. Shiner, C. Trallero-Herrero, N. Kajumba, H. C. Bandulet, D. Comtois, F. Légaré, M. Giguère, J. C. Kieffer, P. B. Corkum, and D. M. Villeneuve, "Wavelength scaling of high harmonic generation efficiency," Phys. Rev. Lett. **103**, 1–4 (2009).
5. I. T. Sorokina, V. V. Dvoyrin, N. Tolstik, and E. Sorokin, "Mid-IR Ultrashort Pulsed Fiber-Based Lasers," IEEE J. Sel. Top. Quantum Electron. **20**, 99-110 (2014).
6. S. B. Mirov, V. V. Fedorov, D. Martyshkin, I. S. Moskalev, M. Mirov, and S. Vasilyev, "Progress in Mid-IR Lasers Based on Cr and Fe-Doped II-VI Chalcogenides," IEEE J. Sel. Top. Quantum Electron. **21**, 292-310 (2015).
7. N. Tolstik, E. Sorokin, and I. T. Sorokina, "Graphene mode-locked Cr:ZnS laser with 41 fs pulse duration.," Opt. Express **22**, 5564–71 (2014).
8. P. Moulton and E. Slobodchikov, "1-GW-Peak-Power, Cr:ZnSe Laser," in *CLEO:2011 - Laser Applications to Photonic Applications* (OSA, 2011), p. PDPA10.
9. S. Duval, M. Bernier, V. Fortin, J. Genest, M. Piche, and R. Vallee, "Femtosecond fiber lasers reach the mid-infrared," Optica **2**, 623–626 (2015).
10. M. Baudisch, H. Pires, H. Ishizuki, T. Taira, M. Hemmer, and J. Biegert, "Sub-4-optical-cycle, 340 MW peak power, high stability mid-IR source at 160 kHz," J. Opt. **17**, 94002 (2015).
11. B. W. Mayer, C. R. Phillips, L. Gallmann, and U. Keller, "Mid-infrared pulse generation via achromatic quasi-phase-matched OPCPA," Opt. Express **22**, 20798–808 (2014).
12. P. Rigaud, A. Van De Walle, M. Hanna, N. Forget, F. Guichard, Y. Zaouter, K. Guesmi, F. Druon, and P. Georges, "Supercontinuum-seeded few-cycle mid-infrared OPCPA system," **24**, 26494–26502 (2016).
13. M. Baudisch, M. Hemmer, H. Pires, and J. Biegert, "Performance of MgO:PPLN, KTA, and $KNbO_3$ for mid-wave infrared broadband parametric amplification at high average power," Opt. Lett. **39**, 5802–5805 (2014).
14. G. Andriukaitis, T. Balčiūnas, S. Ališauskas, A. Pugžlys, A. Baltuška, T. Popmintchev, M.-C. Chen, M. M. Murnane, and H. C. Kapteyn, "90 GW peak power few-cycle mid-infrared pulses from an optical parametric amplifier.," Opt. Lett. **36**, 2755–7 (2011).
15. M. Mero, F. Noack, F. Bach, V. Petrov, and M. J. J. Vrakking, "High-average-power, 50-fs parametric amplifier front-end at 155 μm," Opt. Express **23**, 33157 (2015).
16. J. Boullet, Y. Zaouter, J. Limpert, S. Petit, Y. Mairesse, B. Fabre, J. Higuet, E. Mével, E. Constant, and E. Cormier, "High-order harmonic generation at a megahertz-level repetition rate directly driven by an ytterbium-doped-fiber chirped-pulse amplification system.," Opt. Lett. **34**, 1489–1491 (2009).
17. M. Kienel, M. Müller, A. Klenke, J. Limpert, and A. Tünnermann, "12 mJ kW-class ultrafast fiber laser system using multidimensional coherent pulse addition," Opt. Lett. **41**, 3343 (2016).
18. S. Hädrich, M. Kienel, M. Müller, A. Klenke, J. Rothhardt, R. Klas, T. Gottschall, T. Eidam, A. Drozdy, P. Jójárt, Z. Várallyay, E. Cormier, K. Osvay, A. Tünnermann, and J. Limpert, "Energetic sub-2-cycle laser with 216 W average power," Opt. Lett. **41**, 4332–4335 (2016).
19. a E. Dormidonov, V. O. Kompanets, S. V Chekalin, and V. P. Kandidov, "Gianticallly blue-shifted visible light in femtosecond mid-IR filament in fluorides.," Opt. Express **23**, 29202–10 (2015).
20. F. Silva, D. R. Austin, A. Thai, M. Baudisch, M. Hemmer, D. Faccio, A. Couairon, and J. Biegert, "Multi-octave supercontinuum generation from mid-infrared filamentation in a bulk crystal.," Nat. Commun. **3**, 807 (2012).
21. S. Ališauskas, D. Kartashov, A. Pugzlys, D. Faccio, A. Zheltikov, A. Voronin, and A. Baltuska, "Dispersive Wave Emission by Mid-IR Filaments in Solids," in *CLEO: 2013* (OSA, 2013), p. QW1E.6.
22. M. Durand, A. Houard, K. Lim, A. Durécu, O. Vasseur, and M. Richardson, "Study of filamentation threshold in zinc selenide," Opt. Express **22**, 5852–5858 (2014).
23. A. Choudhuri, A. Ruehl, N. Dipalo, I. Leon, I. Hartl, R. J. D. Miller, and J. Biegert, "Multi-Octave Supercontinuum Generation Driven by Few- Cycle Mid-IR Pulses in YAG , ZnSe And Sapphire," 3–4 (2016).
24. L. Gallmann, "Sources and techniques for attosecond science," ETH Zurich (2011).
25. M. N. Polyanskiy, "Citing RefractiveIndex.INFO," http://refractiveindex.info/about.php.
26. S. Ghimire, A. D. DiChiara, E. Sistrunk, P. Agostini, L. F. DiMauro, and D. A. Reis, "Observation of high-order harmonic generation in a bulk crystal," Nat. Phys. **7**, 138–141 (2011).
27. A. H. Chin, O. G. Calderón, and J. Kono, "Extreme midinfrared nonlinear optics in semiconductors," Phys. Rev. Lett. **86**, 3292–3295 (2001).
28. T. Kanai, P. Malevich, S. S. Kangaparambil, H. Hoogland, and R. Holzwarth, "110-fs , 5- μ m ZGP Parametric Amplifier Driven by a ps Ho : YAG Chirped Pulse Amplifier," 1–2 (n.d.). in *Conference on Lasers and Electro-Optics*, OSA Technical Digest (2016) (Optical Society of America, 2016), paper STu3I.2.
29. T. D. Chinh, W. Seibt, and K. Siegbahn, "Dot patterns from second-harmonic and sum-frequency generation in polycrystalline ZnSe," J. Appl. Phys. **90**, 2612 (2001).
30. L. V. Keldysh, "Ionization in the field of a strong electromagnetic wave," Sov. Phys. JETP **20**, 1307–1314 (1965).
31. G. Vampa, T. J. Hammond, N. Thir??, B. E. Schmidt, F. Légaré, C. R. McDonald, T. Brabec, D. D. Klug, and P. B. Corkum, "All-Optical Reconstruction of Crystal Band Structure," Phys. Rev. Lett. **115**, 1–5 (2015).